Journal of Alloys and Compounds 875 (2021) 159926

Contents lists available at ScienceDirect

Journal of Alloys and Compounds

journal homepage: www.elsevier.com/locate/jalcom

Phase transformations of zircon-type $DyVO_4$ at high pressures up to 36.4 GPa: X-ray diffraction measurements

Xiaoning Wang[a,b,1], Baoyun Wang[a,b,*,1], Dayong Tan[c,d], Wansheng Xiao[c,d], Maoshuang Song[a,d,*]

[a] State Key Laboratory of Isotope Geochemistry, Guangzhou Institute of Geochemistry, Chinese Academy of Sciences, Guangzhou 510640, China
[b] College of Earth and Planetary Sciences, University of Chinese Academy of Sciences, Beijing 100049, China
[c] Key Laboratory of Mineralogy and Metallogeny, Guangzhou Institute of Geochemistry, Chinese Academy of Sciences, Guangzhou 510640, China
[d] CAS Center for Excellence in Deep Earth Science, Guangzhou 510640, China

ARTICLE INFO

Article history:
Received 5 January 2021
Received in revised form 5 April 2021
Accepted 7 April 2021
Available online 20 April 2021

Keywords:
Rare-earth orthovanadates
High pressure
Phase transformation
Angle-dispersive X-ray diffraction

ABSTRACT

The compression behavior of zircon-type $DyVO_4$ has been investigated in a diamond anvil cell by angle-dispersive X-ray diffraction (ADXRD) at high pressures up to 36.4 GPa. Under quasi-hydrostatic compression with argon as the pressure transmitting medium, $DyVO_4$ underwent a sluggish zircon-to-scheelite phase transformation that started at approximately 8.0 GPa and was completed at 15.3 ± 0.9 GPa. The scheelite-type phase remained stable at pressures up to 25.3 GPa and during the process of decompression to ambient conditions, implying that the zircon-to-scheelite transformation is irreversible. Fitting the pressure-volume data using the third-order Birch-Murnaghan equation of state yielded a bulk modulus $B_0 = 129$ (7) GPa and a pressure derivative of bulk modulus $B' = 3.4$ (4) for the zircon-type phase, and $B_0 = 184$ (10) GPa and $B' = 5.3$ (8) for the scheelite-type phase. When compressed in a methanol-ethanol (4:1) pressure transmitting medium, $DyVO_4$ was transformed into the scheelite-type phase at a pressure of 8.8 ± 1.1 GPa and then transformed into a fergusonite-type phase at 21.3 ± 1.6 GPa. The scheelite-to-fergusonite transformation was reversible during decompression. Our study indicates that $DyVO_4$ under compression experiences a sequential zircon-scheelite-fergusonite phase transformation and that the scheelite-fergusonite transformation is sensitive to nonhydrostatic conditions.

1. Introduction

The rare-earth orthovanadates RVO_4 (where R = rare-earth element) have attracted great interest because of their technological applications and theoretical importance in materials science. These compounds are widely exploited as catalysts and laser host materials [1–5]. In particular, due to their excellent luminesce and physical-chemical stability, they are also promising candidates for displays and optical communications and medical applications [6–8]. Under ambient conditions, they usually crystallize in zircon-type structure (space group: $I4_1/amd$ and $Z = 4$) with the exception of $LaVO_4$, which adopts either a zircon-type structure or a monazite-type structure (space group: $P2_1/n$ and $Z = 4$) depending on the growth conditions [9,10]. It is generally accepted that the electronic, optical and thermodynamic properties of materials are closely associated with their crystal structures, which can be regulated by pressure. Therefore, a number of experimental and theoretical studies have been conducted in recent decades to investigate the compression behavior of RVO_4 orthovanadates [11–26]. These studies show that applying pressure leads to structural transformations, insulator-metal transitions and electronic band-gap reduction of RVO_4 compounds.

$DyVO_4$ is a member of the rare-earth orthovanadate RVO_4 family. It has been investigated by many researchers for its Jahn–Teller distortion and giant magnetocaloric effect [27–30]. Recent studies have focused on its photocatalytic properties for splitting water and degrading organic compounds [31–33]. However, in contrast to other rare-earth orthovanadates, relatively few high-pressure studies have been carried out on $DyVO_4$. Thirty years ago, Duclos et al. observed an irreversible phase transformation of $DyVO_4$ from zircon-type structure to scheelite-type structure at 6.5 GPa using Raman

* Corresponding authors at: State Key Laboratory of Isotope Geochemistry, Guangzhou Institute of Geochemistry, Chinese Academy of Sciences, Guangzhou 510640, China.
E-mail addresses: wangbaoyun@gig.ac.cn (B. Wang), msong@gig.ac.cn (M. Song).
[1] These authors contributed equally to this work.

https://doi.org/10.1016/j.jallcom.2021.159926
0925-8388/

scattering spectroscopy [34]. The zircon-to-scheelite phase transformation of $DyVO_4$ was also confirmed by a later Raman scattering study but was found to occur at approximately 8 GPa [35]. Until now, only one high-pressure XRD study has been reported for $DyVO_4$ [20]. Paszkowicz et al. [20] conducted energy-dispersive X-ray diffraction measurements on synthesized zircon-type and scheelite-type phases of $DyVO_4$ at pressures up to 8.44 GPa using a multi-anvil press. They employed Vaseline as a pressure transmitting medium that maintained pseudohydrostatic conditions up to approximately 6 GPa, and used XRD data obtained below 6 GPa to determine the equations of state for both phases. Hence, further in-situ XRD experiments run over a wide pressure range are still needed to shed light on the structural evolution of $DyVO_4$ across the zircon-scheelite transformation and probe whether a new phase could emerge after the scheelite-type phase. Bastide proposed a two-dimensional diagram that correlates the crystal structures of ABX_4 ternary compounds with the ionic radius ratios r_A/r_X and r_B/r_X [36]. Bastide's diagram indicates that the pressure-induced phase transition sequence of an ABX_4 compound follows the so-called northeast (NE) rule and occurs in the direction in which both r_A/r_X and r_B/r_X values increase simultaneously. Such a NE rule has been verified with many tungstates and orthovanadates [37,38]. It can reasonably be predicted that scheelite-type $DyVO_4$ will transform to the fergusonite structure under high pressure.

Motivated by the issues mentioned above, we performed synchrotron angle-dispersive X-ray diffraction (ADXRD) measurements at high pressures up to 36.4 GPa on orthovanadate $DyVO_4$. Our experiments extended the pressure range covered by previous Raman and XRD experiments [20,34,35], allowing us to investigate the pressure-induced structural evolution of $DyVO_4$ and seek new high-pressure polymorphs. The aim of this work is to observe the zircon-scheelite transformation in situ, probe the possible existence of the fergusonite phase, and determine the evolution of lattice parameters and the equations of state for the $DyVO_4$ polymorphs. In particular, the effect of hydrostaticity on the phase transformations is also evaluated.

2. Experimental details

Polycrystalline $DyVO_4$ was synthesized by the solid-state reaction of stoichiometric amounts of Dy_2O_3 and V_2O_5. A homogeneous mixture of Dy_2O_3 and V_2O_5 powders placed in a platinum crucible was heated at 1073 K for 12 h, subsequently heated at 1373 K for another 12 h in an electrical furnace, and then cooled to room temperature naturally. By means of X-ray diffraction measurements, the synthesized product was verified to be a pure zircon-type phase of $DyVO_4$. The unit-cell parameters were determined to be $a = b = 7.1540(3)$ Å, $c = 6.3136$ (4) Å, and $V = 323.13(2)$ Å^3, which are very consistent with the values reported in the literature [39].

Angle-dispersive X-ray diffraction (ADXRD) measurements were performed on zircon-type $DyVO_4$ at high pressure to investigate its compression behavior. Pressure was generated by a symmetric Mao-Bell type diamond-anvil cell (DAC) with a culet size of 300 µm. Powder samples approximately 15 µm in thickness and 50 µm in diameter were loaded into the sample chamber, a 100 µm-diameter hole in a T301 steel gasket preindented to a thickness of 45 µm. Two series of in situ high-pressure ADXRD experiments were conducted: one up to 25.3 GPa with argon employed as pressure transmitting medium (Ar experiments) and the other up to 36.4 GPa with a mixture of methanol–ethanol (ME) in a 4:1 ratio as the pressure transmitting medium (ME experiments). The argon experiments were performed with an incident monochromatic X-ray wavelength of 0.6199 Å and a focused beam size of approximately 20 × 10 µm^2 at the 4W2 beamline of the Beijing Synchrotron Radiation Facility (BSRF), and the two-dimensional diffraction patterns were recorded with an exposure time of 10 min using an image plate detector

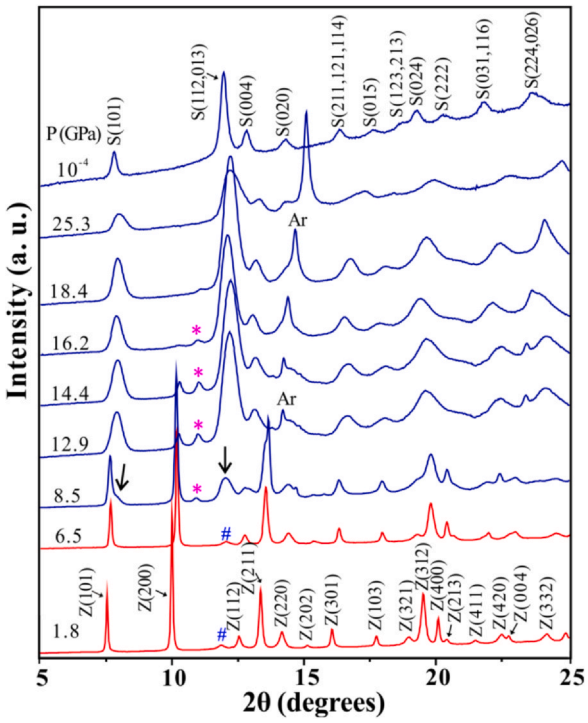

Fig. 1. Angle-dispersive X-ray diffraction patterns collected at various pressures for the experiments with argon as the pressure transmitting medium. Weak diffraction peaks of the scheelite-type phase (marked by arrows) appear in the 8.5 GPa pattern and the peaks of the zircon-type phase disappear in the 16.2 GPa pattern. The pound symbols (#) denote the diffraction peaks for the minor impurity of the scheelite-type phase. The asterisks (*) denote the diffraction peaks for the impurity of V_2O_5.

(MAR-345). The experiments with the ME pressure medium were conducted with a wavelength of 0.6199 Å and a focused beam size of approximately 5 × 5 µm^2 at beamline 15U1 of the Shanghai Synchrotron Radiation Facility (SSRF), and the two-dimensional diffraction patterns were recorded with an exposure time of 40 s using a Mar-165 charge-coupled device (CCD) detector. Ruby fluorescence and platinum pressure scales were applied to determine pressures for the experiments with argon and ME pressure mediums, respectively [40,41]. For both series of experiments, the distances between the sample and detector and the orientations of the detector were calibrated by using CeO_2 as a standard. The two-dimensional diffraction images were integrated with the Fit2D and Dioptas programs to obtain one-dimensional diffraction patterns of intensity versus 2θ [42,43]. The LeBail refinements of structural parameters were performed using the GSAS software package [44].

3. Results and discussion

Representative angle-dispersive X-ray diffraction patterns of $DyVO_4$ collected from the experiments with the argon pressure medium are shown in Fig. 1. The diffraction pattern at 1.8 GPa can be indexed well to a zircon-type structure. A weak peak marked by the pound symbol (#) at approximately 12º indicates that a small amount of impurity exists, which can be assigned to the scheelite-type phase of $DyVO_4$ probably produced during the process of sample preparation. $DyVO_4$ was found to maintain its zircon-type structure at pressures up to 6.5 GPa as no significant changes were observed except for a slight shift and broadening of diffraction peaks with pressure. At 8.5 GPa, the diffraction pattern shows that several new but weak diffraction peaks, as marked by short arrows, began to appear, indicating transformation into a new phase. We estimate that the onset of the phase transformation is at around 8.0 GPa. Under further compression, the intensities of the diffraction peaks

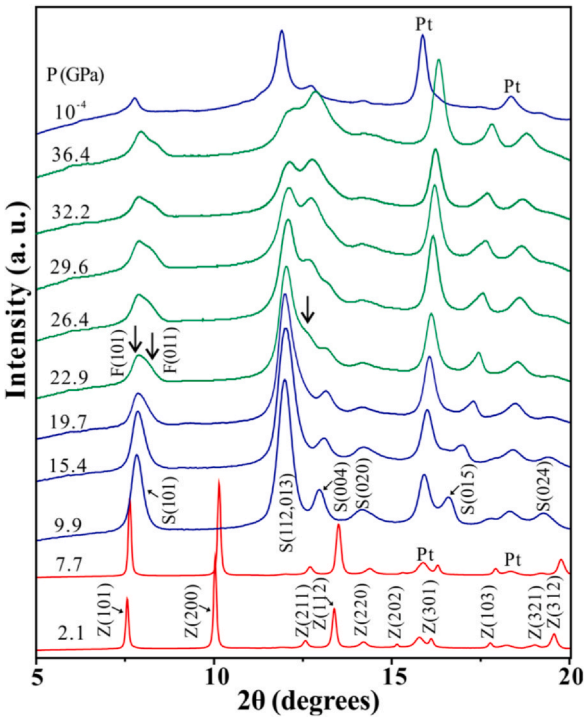

Fig. 2. Angle-dispersive X-ray diffraction patterns collected at various pressures for the experiments with 4:1 methanol-ethanol mixture as the pressure transmitting medium. The zircon-scheelite phase transformation occurs as the pressure increases from 6.5 GPa to 8.5 GPa. The diffraction peaks marked by arrows in the 22.9 GPa pattern indicate a transformation into the fergusonite-type phase.

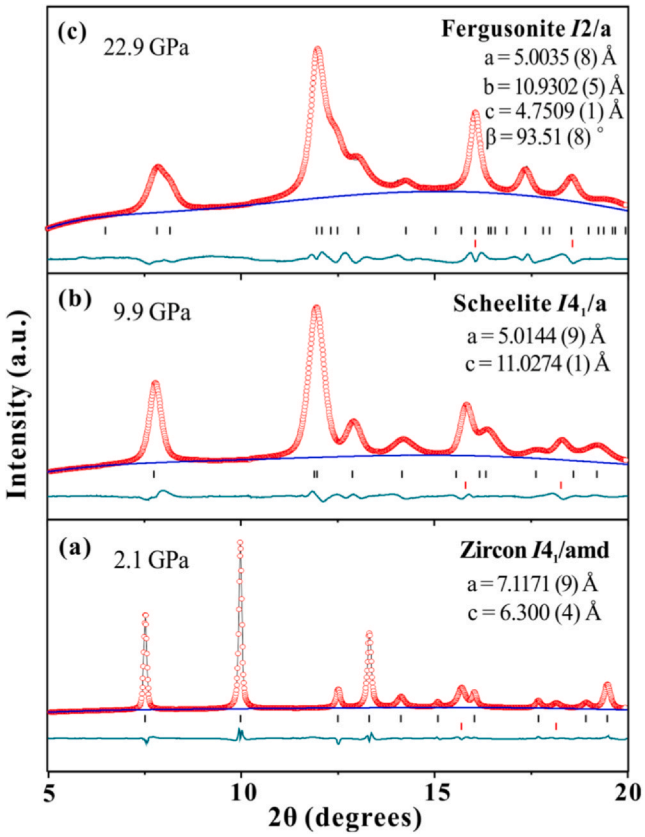

Fig. 3. LeBail refinements of the diffraction patterns for various phases of $DyVO_4$: (a) zircon-type phase at 2.1 GPa (b) scheelite-type phase at 9.9 GPa; (c) fergusonite-type phase at 22.9 GPa. Experimental diffraction patterns are represented by red circles; black, blue and dark cyan solid lines represent refined diffraction patterns, backgrounds and residuals respectively. Black and red vertical ticks indicate the calculated Bragg reflections of $DyVO_4$ and Pt respectively.

for the zircon-type phase decreased while the intensities of the diffraction peaks for the new phase increased gradually. In the 16.2 GPa diffraction pattern, all the typical diffraction peaks of the $DyVO_4$ zircon-type phase disappeared completely, implying that the phase transformation was completed. We estimate that the phase transformation ends at 15.3 ± 0.9 GPa. The new phase persists up to the maximum pressure of 25.3 GPa and can be decompressed to ambient conditions as the diffraction patterns at the two pressures are nearly identical.

Fig. 2 displays representative diffraction patterns of $DyVO_4$ measured up to 36.4 GPa for the experiments with the ME pressure medium. The diffraction patterns at pressures below 6.6 GPa exhibit no obvious changes, and all the diffraction peaks except for two peaks of the platinum (Pt) pressure marker can be indexed to the zircon-type structure (space group $I4_1/amd$). This was also confirmed by a LeBail refinement of the diffraction pattern at 2.1 GPa, which yielded lattice parameters $a = 7.1171(9)$ Å and $c = 6.300(4)$ Å, as shown in Fig. 3(a). When the pressure was increased to 9.7 GPa, significant and discontinuous changes were observed; these are similar to those seen during the phase transformation from the zircon-type phase to a new phase in the argon experiments, in that a few new diffraction peaks appeared, and these peaks of the zircon-type phase vanished. In the diffraction pattern at 9.7 GPa, most diffraction peaks can be assigned to the scheelite-type structure (space group $I4_1/a$) except for two peaks of Pt. The LeBail refinement shown in Fig. 3(b) also confirms that the 9.7 GPa diffraction pattern corresponds to a scheelite-type structure with no zircon-type phase, yielding unit-cell lattice parameters $a = 5.0144(9)$ Å and $c = 11.0274(1)$ Å. Hence, when pressure was increased from 7.7 GPa to 9.9 GPa, $DyVO_4$ was fully converted from the zircon-type phase into the scheelite-type phase. The scheelite-type phase remained stable up to 19.7 GPa. It is worth noting that the diffraction peaks of the scheelite-type phase are much broader than those of the zircon-type phase. A similar phenomenon has been reported for other orthovanadates, such as $SmVO_4$ and $HoVO_4$ [19,23], and such a significant peak broadening of the scheelite-type phase is taken as an intrinsic property of these materials. It is expected that the zircon-scheelite structural transformation need to overcome high energy barrier and that many defects are introduced in the system during transition.

The scheelite-type phase of $DyVO_4$ was stable at pressures between 9.7 GPa and 19.7 GPa and showed no obvious broadening of its diffraction peaks with pressure. Under compression to pressures beyond 19.7 GPa, the diffraction peaks began to broaden and some new peaks, marked by short arrows, emerged in the diffraction pattern at 22.9 GPa. These changes are consistent with a scheelite-to-fergusonite phase transformation, which has been reported for some other orthovanadates [45]. In particular, the (101) diffraction peak of the scheelite-type phase ($2\theta \approx 8.0°$) in the 19.7 GPa diffraction pattern split into the (101) and (011) peaks of the fergusonite-type phase in the 22.9 GPa diffraction pattern, and the strongest peak at $2\theta \approx 12.0°$ (identified as the (112) and (103) diffraction lines of the scheelite-type phase) became strongly asymmetrical at 22.9 GPa as a consequence of the appearance of new diffraction peaks for the fergusonite-type phase. A LeBail refinement of the diffraction pattern at 22.9 GPa further confirmed the fergusonite-type structure (Fig. 3(c)), and yielded the unit-cell lattice parameters $a = 5.0035(8)$ Å, $b = 10.9302(0)$ Å, $c = 4.7509(1)$ Å and $\beta = 93.51(8)$ Å. The fergusonite-type phase remained stable up to 36.4 GPa, the maximum pressure for the experiments with the ME pressure medium. When the pressure was released to ambient conditions, the fergusonite-type phase reverted into the scheelite-type phase; this indicates that the scheelite-to-fergusonite phase transformation is

reversible, but the zircon-to-scheelite phase transformation is irreversible.

By comparison with the experiments with the ME pressure medium, the phase transformation at approximately 8.0 GPa observed for the experiments with an argon pressure medium can also be assigned to the zircon-to-scheelite phase transformation; the variations in diffraction patterns across the phase transformations for both series of experiments were nearly identical. For the experiments with an argon pressure medium, the zircon-to-scheelite phase transformation started at approximately 8.0 GPa and was completed at approximately 15.3 ± 0.9 GPa, implying that zircon-type and scheelite-type phases coexist over a wide span of pressure. For the experiments with an ME pressure medium, however, the pressure span for the coexistence of the two phases was much narrower as the zircon-to-scheelite phase transformation initiated and was completed when the pressure increased from 7.7 GPa to 9.9 GPa. Using argon as a pressure transmitting medium provided quasi-hydrostatic environments up to a maximum pressure of 25.3 GPa; however, using a 4:1 methanol-ethanol mixture as a pressure transmitting medium can guarantee quasi-hydrostatic conditions only up to approximately 10 GPa [46]. This means that the pressure range for coexistence of the two phases in the zircon-to-scheelite phase transformation can be affected by the selection of the pressure transmitting medium. In addition, the scheelite-to-fergusonite phase transformation seems to be sensitive to non-hydrostatic conditions as we observed this phase transformation only for the experiments with an ME pressure medium.

To extract the unit-cell parameters of the three $DyVO_4$ phases, we performed LeBail refinements on the diffraction patterns collected in this study. The pressure evolution of the unit-cell parameters of $DyVO_4$ is depicted in Fig. 4. The lattice parameters of the zircon-type, scheelite-type and fergusonite-type phases show an approximately linear relationship with pressure. For the experiments with the ME pressure medium, the nonhydrostaticity of the methanol-ethanol pressure transmitting medium at pressures above 10 GPa resulted in that diffraction data that are not of high quality; hence, we mainly analyze the diffraction data collected from the experiments with the argon pressure medium in this study. The lattice parameters of the zircon-type and scheelite-type phases for the experiments with an argon pressure medium can be fitted as a linear function of pressure as follows:

Zircon-type phase: $a = 7.147(6) - 1.77(1) \times 10^{-2}P$

$c = 6.308(9) - 1.08(8) \times 10^{-2}P$

Scheelite-type phase: $a = 5.058(4) - 5.8(3) \times 10^{-3}P$

$c = 11.237(6) - 1.87(3) \times 10^{-2}P$

Both the zircon-type and scheelite-type phases show anisotropic axial compression behavior. For the zircon-type phase, the *a*-axis is more compressible than the *c*-axis, as indicated by the linear compressibilities of lattice parameters *a* and *c*, $Ka = 1.77 \times 10^{-2}$ GPa and $Kc = 1.08 \times 10^{-2}$ Å/GPa. For the scheelite-type phase, however, the *c*-axis becomes more compressible than the *a*-axis as indicated by its compressibility values $Ka = 0.58 \times 10^{-2}$ GPa and $Kc = 1.87 \times 10^{-2}$ Å/GPa. The difference in anisotropic compression behavior between the zircon-type and scheelite-type phases is also reflected in their dependence on pressure, which shows a monotonic increase in the *c/a* ratio with pressure for the zircon-type phase but a monotonic decrease in the *c/a* ratio with pressure for the scheelite-type phase. Similar anisotropic axial compression behavior has been reported for some compounds in the RVO_4 family [12]. For the fergusonite-type phase, it is found that the lattice parameters *a* and *c* are close to the value of lattice parameter *a* for the scheelite-type phase. The β is approximately 90 degrees and gradually shifts to higher angles under compression.

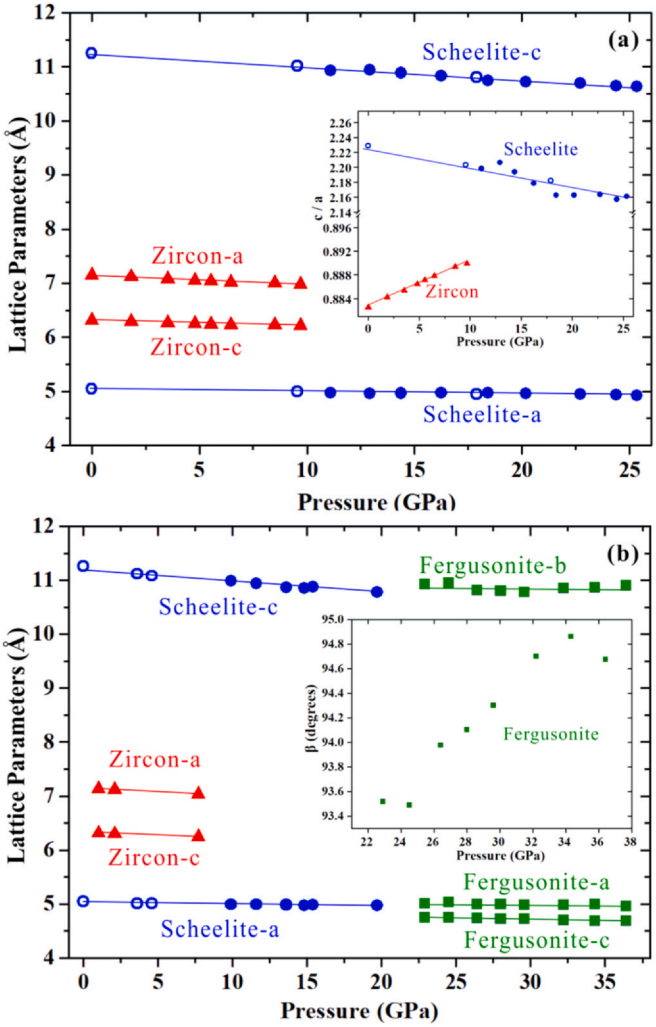

Fig. 4. Pressure dependence of the lattice parameters for various $DyVO_4$ phases: (a) Ar experiments, the inset shows the variations of c/a ratio as a function of pressure for zircon-type and scheelite-type phases; (b) ME experiments, the inset shows the evolution of monoclinic angle β in the fergusonite-type phase. Solid symbols denote the compression data , while open symbols denote decompression data. Solid lines are linear fitting results of the data.

The unit-cell volumes were calculated from the unit-cell parameters at each pressure and plotted as a function of pressure in Fig. 5. It is obvious that the zircon-to-scheelite phase transformation can be characterized as a first-order transition accompanying a volume collapse approximately 9.1%. However, the volume change for the scheelite-to-fergusonite phase transformation is much smaller. We analyzed pressure-volume (P-V) data with the third-order Birch-Murnaghan equation of state, as follows [47,48]:

$$P(V) = \frac{3B_0}{2}\left[\left(\frac{V_0}{V}\right)^{7/3} - \left(\frac{V_0}{V}\right)^{5/3}\right]\left\{1 + \frac{3}{4}(B' - 4)\left[\left(\frac{V_0}{V}\right)^{2/3} - 1\right]\right\}$$

where B_0 and V_0 are the bulk modulus and unit-cell volume at ambient pressure respectively, and $B'$is the pressure derivative of the bulk modulus. To avoid the significant influence of deviatoric stress, we only fitted the pressure-volume data for the experiments run with an argon pressure medium. The best least squares fitting yielded the bulk modulus $B_0 = 129(7)$ GPa and the pressure derivative of the bulk modulus $B' = 3.4$ (4) for the zircon-type phase, and $B_0 = 184(10)$ GPa and $B' = 5.3$ (8) for the scheelite-type phase. We noticed that the pressure-volume data points for the experiments with the ME pressure medium agreed well with the fitted lines from

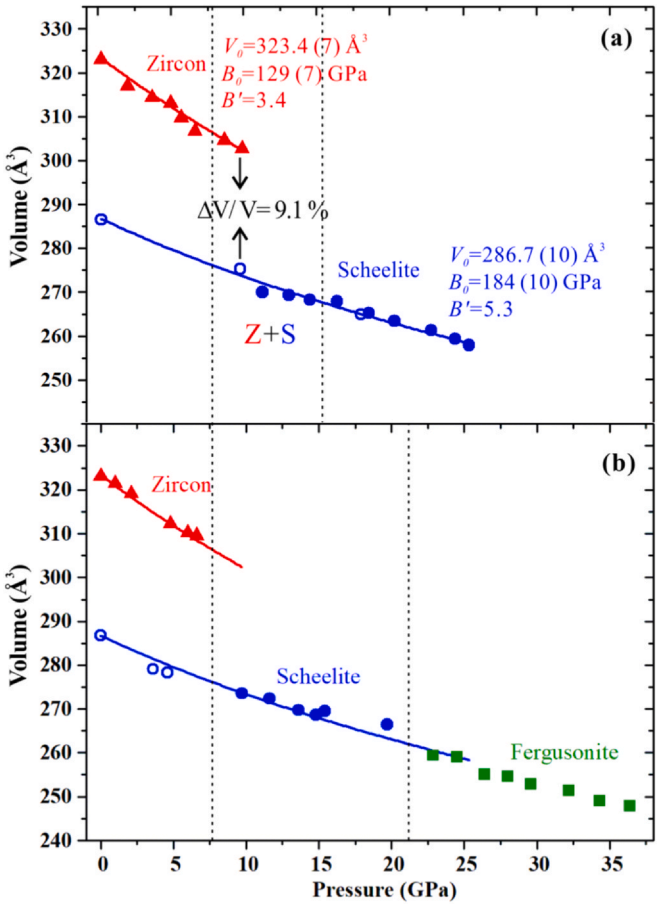

Fig. 5. Pressure dependence of the unit-cell volume for various $DyVO_4$ phases: (a) Ar experiments; (b) ME experiments. Solid and open symbols represent the compression and decompression data respectively. The solid lines represent the fitting results of the data for the Ar experiments using the third-order Birch-Murnaghan equation of state.

Table 1
Experimental results of the bulk modulus and its pressure derivative for the zircon-type and scheelite-type phases for RVO_4 orthovanadates with small rare-earth cations. The pressure transmitting mediums (PTM) are also indicated (MEW: methanol-ethanol-water; ME: methanol-ethanol; Ar: argon; He: helium).

RVO_4	Zircon		Scheelite		PTM	Ref.
	B_0 (GPa)	B'	B_0 (GPa)	B'		
$SmVO_4$	129	4	133	4	MEW	[23]
$EuVO_4$	150	5.3	195	5.5	ME	[21]
$GdVO_4$	122	4.2	137	6	Ar	[25]
$TbVO_4$	122	6.2	163	5.8	Ar	[14]
$DyVO_4$	118	4.6	153	4.2	Vaseline	[20]
	129.2	3.4	184.2	5.3	Ar	This work
$HoVO_4$	160	5	180	5.5	ME	[19]
$ErVO_4$	158	4	158	4	ME	[26]
$TmVO_4$	120	4	131.8	4	He	[24]
$YbVO_4$	141	4	159	4	ME	[13]
$LuVO_4$	147	4.3	194	5.3	ME	[11]

the Birch-Murnaghan equation of state for the experiments done with the argon pressure medium but deviated from the fitted line of the scheelite-type phase at pressures above approximately 12 GPa; this is probably due to the nonhydrostaticity of the ME pressure medium. The obtained values of the bulk modulus and its pressure derivative of $DyVO_4$ are summarized in Table 1, together with those for other RVO_4 orthovanadates with small rare-earth cations. The bulk modulus values of the zircon-type and scheelite-type phases of $DyVO_4$ determined in this study are higher than the values reported by Paszkowicz et al. [20]. This may be attributed to the use of Vaseline as a pressure transmitting medium in their experiments, which limited pseudohydrostatic conditions to pressures only below 6 GPa. We note that our bulk modulus value for the zircon-type phase is very close to those of $SmVO_4$, $GdVO_4$, $TbVO_4$ and $TmVO_4$, but is smaller than those of $EuVO_4$, $HoVO_4$, $ErVO_4$, $YbVO_4$ and $LuVO_4$. Our bulk modulus value for the scheelite-type $DyVO_4$ phase is close to that of $HoVO_4$, slightly lower than those of $EuVO_4$ and $LuVO_4$, but higher than those of $SmVO_4$, $GdVO_4$, $TbVO_4$, $ErVO_4$, $TmVO_4$, and $YbVO_4$. It seems that there exists no obvious correlation between the bulk modulus and rare-earth cation radius, especially for the scheelite-type phase. Our present experiments and previous experimental studies on rare-earth orthovanadates employed various pressure transmitting mediums, including argon, helium, methanol-ethanol mixture (ME, 4:1 in ratio) and methanol-ethanol-water mixture (MEW, 16:3:1 in ratio). Klotz et al. (2009) investigated the hydrostaticity of common pressure mediums, and found that ME and MEW are nonhydrostatic at high pressures above 10 GPa [46]. Therefore, the bulk modulus values determined in the present and previous studies may be affected more or less by pressure transmitting mediums, especially for the scheelite-type phase which is stable at pressures from approximately 8 to 20 GPa. In this regard, using noble-gases such as He, Ne and Ar, which are known to provide excellent hydrostatic conditions at very high pressure, as pressure transmitting mediums, will be more reasonable for the acquisition of precise parameters for the equation of state. However, according to previous studies, the transition to a fergusonite-type phase is triggered by the existence of deviatoric stress, which requires the use a nonhydrostatic pressure transmitting medium. For instance, Garg et al. reported that fergusonite-type $HoVO_4$ appeared at 23 GPa when ME was applied as a pressure transmitting medium, whereas the scheelite-type phase was stable up to 28 GPa when argon was used as a pressure transmitting medium [19]. Recently, $ScVO_4$ was found to transform directly from zircon-type to fergusonite-type phases under nonhydrostatic compression without undergoing the scheelite-type phase [49]. Therefore, nonhydrostatic pressure transmitting mediums such as ME and MEW are still important for probing high-pressure polymorphs and phase transformations of rare-earth orthovanadates and other compounds.

Our ADXRD experiments on zircon-type $DyVO_4$ at pressures up to 36.4 GPa certified that $DyVO_4$ under compression follows the zircon-scheelite-fergusonite structural sequence. The crystal structures of these three polymorphs are depicted in Fig. 6. The zircon-to-scheelite phase transformation took place at approximately 8.0 GPa and was accompanied by a volume reduction of approximately 9.1%. Although both the zircon-type and scheelite-type phases belong to the same tetragonal crystal system, they showed opposite axial compressibility behaviors, which can be attributed to their respective crystal structures. As seen in Fig. 6, both phases are composed of two types of basic structural (polyhedral) units, VO_4 tetrahedra and DyO_8 dodecahedra, but the arrangements of the two types of units in the two phases are significantly different. In the zircon-type phase, alternating edge-sharing VO_4 tetrahedra and DyO_8 dodecahedra form chains parallel to the crystallographic *c*-axis. Each of these chains is connected laterally through edge-sharing DyO_8 dodecahedra along the *a*-axis direction. Many previous studies on zircon-type RVO_4 compounds revealed that the RO_8 dodecahedra are more compressible than the VO_4 tetrahedra [12], which makes the *a*-axis more compressible than the *c*-axis. Accordingly, the anisotropic axial compressibility of zircon-type $DyVO_4$ can be explained by considering its specific crystal structure. However, in the scheelite-type phase, chains composed of alternating VO_4 tetrahedra and DyO_8 dodecahedra are arranged in directions parallel to the *a*-*b* plane and linked by corner-sharing DyO_8 dodecahedra along the *c*-axis. Therefore, the scheelite-type phase shows that the compressibility in the *c*-axis is higher than that in the *a*-axis,

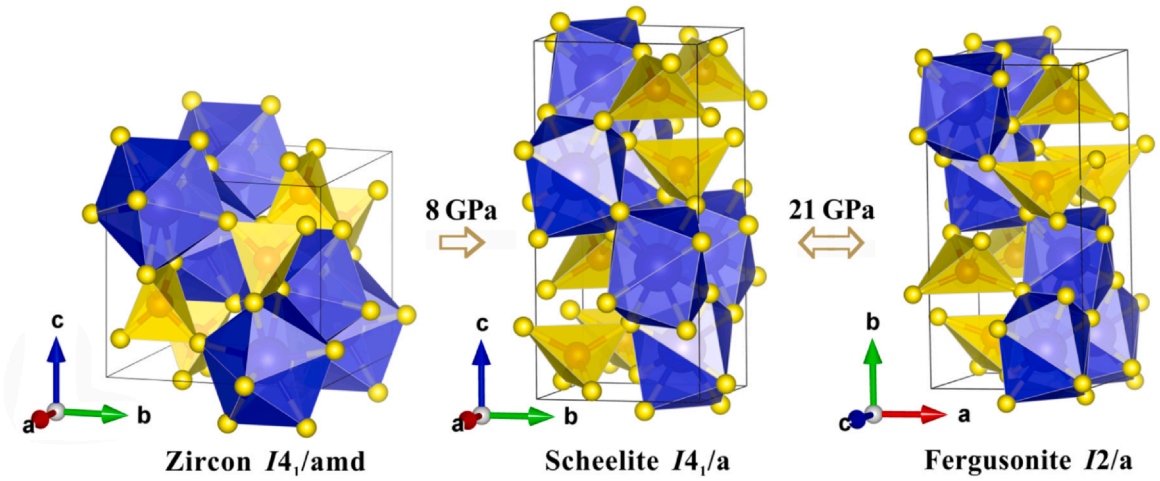

Fig. 6. Crystal structures of the zircon-type ($I4_1/amd$, $Z = 4$), scheelite-type ($I4_1/a$, $Z = 4$) and fergusonite-type ($I2/a$, $Z = 4$) polymorphs of $DyVO_4$. Large blue, medium red and small yellow spheres represent Dy, V and O atoms, respectively. VO_4 tetrahedra and DyO_8 dodecahedra units are displayed. The unit cells are shown with fine solid lines. The phase transition pressures are also indicated.

exhibiting completely different axial compressibilities than the zircon-type phase.

Finally, we summarize the compression behaviors of zircon-type rare-earth RVO_4 orthovanadates which have been investigated by X-ray diffraction and Raman scattering spectroscopy measurements [11,13–16,18,19,21–26,35], as illustrated in Fig. 7. Orthovanadates with rare-earth R cations of large radius, e.g., La-Ce, exhibit sequential zircon-monazite-post-monazite phase transformations under compression. The crystal structure of the post-monazite phase has not yet been determined due to its low symmetry which leads to the overlap of diffraction lines in the powder X-ray diffraction pattern. Orthovanadates with small rare-earth R cations, e.g., Sm-Lu, undergo an irreversible zircon-to-scheelite phase transformation with onset pressures of approximately 4–8 GPa. The pressure ranges for coexistence of the zircon-type and scheelite-type phases for Ho, Er, Tm, Yb and Lu orthovanadates are obviously wider than those for orthovanadates with other rare-earth cations. With further compression, the scheelite-type phase transforms into the fergusonite-type phase. The pressure of the scheelite-to-fergusonite transformation is sensitive to the ionic radius of the rare-earth cation. Orthovanadates with large rare-earth cations (e.g. Tb, Dy and Ho) show higher scheelite-to-fergusonite transformation pressures than those with small rare-earth cations (e.g. Lu). By taking into account all the experimental results of the zircon-type rare-earth RVO_4 orthovanadates and the similarities of the lanthanide elements, we postulate that the zircon-scheelite-fergusonite structural sequence is a general rule for the pressure-induced structural evolution for all orthovanadates with small rare-earth cations [45]. Therefore, it can be reasonably expected that scheelite-to-fergusonite transformation may also take place with $ErVO_4$, $TmVO_4$ and $SmVO_4$, which has not yet been confirmed.

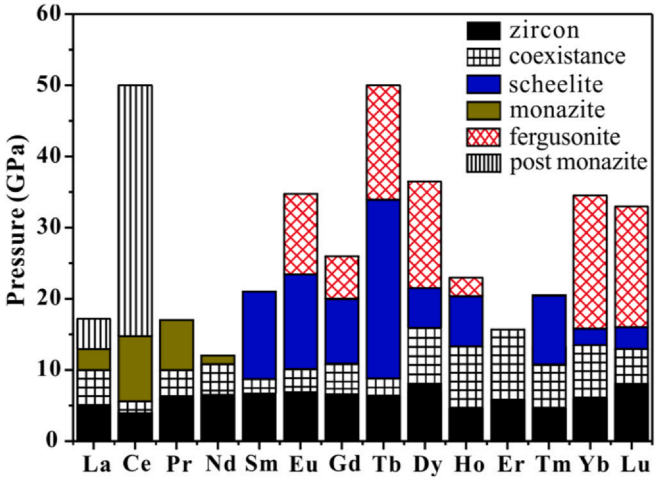

Fig. 7. Schematic diagram of the high-pressure phase transformations for zircon-type rare-earth orthovanadates. Bars represent pressure ranges of the formation of different phases determined in the compression process. Data for $DyVO_4$ are from present work, and the data for other orthovanadates are collected from the literature [11,13–16,18,19,21–26,35].

4. Conclusions

In summary, the compression behavior of $DyVO_4$ has been investigated by in situ ADXRD measurements at high pressures up to 36.4 GPa. Two series of experiments were conducted, one with argon as the pressure transmitting medium and the other with a methanol-ethanol mixture as the pressure transmitting medium. The successive sequence of zircon-scheelite-fergusonite phase transformations was clearly observed. The irreversible phase transformation from zircon-type to scheelite-type structure take place at approximately 8.0 GPa. The reversible scheelite-to-fergusonite phase transformation takes place at approximately 21.3 ± 1.6 GPa and is sensitive to nonhydrostatic conditions. The pressure-volume data obtained from the experiments with an argon pressure medium were fitted by the third-order Birch-Murnaghan equation of state, which yielded a bulk modulus $B_0 = 129$ (7) GPa and a pressure derivative of the bulk modulus $B' = 3.4$ (4) for the zircon-type phase, and $B_0 = 184$ (10) GPa and $B' = 5.3$ (8) for the scheelite-type phase. Our study indicates that $DyVO_4$ under compression experiences a sequential zircon-scheelite-fergusonite phase transformation, and the scheelite-fergusonite transformation is sensitive to nonhydrostatic condition. The high-pressure phase behavior of $DyVO_4$ observed in this study is in good agreement with those of other rare-earth orthovanadates with rare-earth cations with small radii reported in previous studies [45], implying that the sequence of zircon-scheelite-fergusonite phase transformations might be a common path of pressure-induced structural evolution for these orthovanadates.

CRediT authorship contribution statement

Maoshuang Song and Baoyun Wang designed the project. Baoyun Wang and Xiaoning Wang conducted the high-pressure XRD

measurements and data analysis. Dayong Tan and Wansheng Xiao provided advices on this project. Baoyun Wang: Writing - original draft. All authors reviewed the manuscript.

Declaration of Competing Interest

We declare that we have no known competing financial interests or personal relationships that could have appeared to influence the work reported in this paper.

Acknowledgments

Wei Zhou is thanked for helping during high-pressure ADXRD experiments and some data processing work. High-pressure XRD experiments were carried out at the BL15U1 beamline of Shanghai Synchrotron Radiation Facility (SSRF) and the 4W2 High Pressure Beamline of Beijing Synchrotron Radiation Facility (BSRF). This research was financially supported by the Strategic Priority Research Program (B) of the Chinese Academy of Sciences (Grant no. XDB18000000) and the National Natural Science Foundation of China (Grants nos. 41874107, 41574079). This is Contribution no. IS-3008 from GIGCAS.

References

[1] T. Li, L. Zhao, Y. He, J. Cai, M. Luo, J. Lin, Synthesis of g-C_3N_4/$SmVO_4$ composite photocatalyst with improved visible light photocatalytic activities in RhB degradation, Appl. Catal. B: Environ. 129 (2013) 255–263.
[2] X. Zhao, L. Huang, H. Li, H. Hu, X. Hu, L. Shi, D. Zhang, Promotional effects of zirconium doped $CeVO_4$ for the low-temperature selective catalytic reduction of NOx with NH_3, Appl. Catal. B: Environ. 183 (2016) 269–281.
[3] S. Sun, H. Yu, Y. Wang, H. Zhang, J. Wang, Thermal, spectroscopic and laser characterization of monoclinic vanadate Nd:$LaVO_4$ crystal, Opt. Express 21 (2013) 31119.
[4] R.M. Mohamed, F.A. Harraz, I.A. Mkhalid, Hydrothermal synthesis of size-controllable Yttrium Orthovanadate (YVO_4) nanoparticles and its application in photocatalytic degradation of direct blue dye, J. Alloy. Compd. 532 (2012) 55–60.
[5] J. Gao, X. Yu, F. Chen, X. Li, R. Yan, K. Zhang, J. Yu, Y. Wang, 12.0-W continuous-wave diode-end-pumped Nd:$GdVO_4$ laser with high brightness operating at 912-nm, Opt. Express 17 (2009) 3574–3580.
[6] A. Shyichuk, R.T. Moura, A.N.C. Neto, M. Runowski, M.S. Zarad, A. Szczeszak, S. Lis, O.L. Malta, Effects of dopant addition on lattice and luminescence intensity parameters of Eu(III)-doped lanthanum orthovanadate, J. Phys. Chem. C 120 (2016) 28497–28508.
[7] M. Abdesselem, M. Schoeffel, I. Maurin, R. Ramodiharilafy, G. Autret, O. Clement, P.L. Tharaux, J.P. Boilot, T. Gacoin, C. Bouzigues, A. Alexandrou, Multifunctional rare-Earth vanadate nanoparticles: luminescent labels, oxidant sensors, and MRI contrast agents, ACS Nano 8 (2014) 11126–11137.
[8] V. Tamilmani, A. Kumari, V.K. Rai, B. Unni Nair, K.J. Sreeram, Bright Green frequency upconversion in catechin based Yb^{3+}/Er^{3+} codoped $LaVO_4$ nanorods upon 980 nm excitation, J. Phys. Chem. C 121 (2017) 4505–4516.
[9] B.C. Chakoumakos, M.M. Abraham, L.A. Boatner, Crystal structure refinements of Zircon-type M VO_4 (M = Sc, Y, Ce, Pr, Nd, Tb, Ho, Er, Tm, Yb, Lu), J. Solid State Chem. 109 (1994) 197–202.
[10] C.J. Jia, L.D. Sun, L.P. You, X.C. Jiang, F. Luo, Y.C. Pang, C.H. Yan, Selective Synthesis of Monazite- and Zircon-Type $LaVO_4$ Nanocrystals, Cheminform 109 (2005) 3284–3290.
[11] R. Mittal, A.B. Garg, V. Vijayakumar, S.N. Achary, A.K. Tyagi, B.K. Godwal, E. Busetto, A. Lausi, S.L. Chaplot, Investigation of the phase stability of $LuVO_4$ at high pressure using powder x-ray diffraction measurements and lattice dynamical calculations, J. Phys.: Condens. Matter 20 (2008) 075223.
[12] D. Errandonea, R. Lacomba-Perales, J. Ruiz-Fuertes, A. Segura, S.N. Achary, A.K. Tyagi, High-pressure structural investigation of several zircon-type orthovanadates, Phys. Rev. B 79 (2009) 184104.
[13] A.B. Garg, R. Rao, T. Sakuntala, B.N. Wani, V. Vijayakumar, Phase stability of $YbVO_4$ under pressure: in situ x-ray and Raman spectroscopic investigations, J. Appl. Phys. 106 (2009) 063513.
[14] D. Errandonea, R.S. Kumar, S.N. Achary, A.K. Tyagi, In situhigh-pressure synchrotron x-ray diffraction study of $CeVO_4$ and $TbVO_4$ up to 50 GPa, Phys. Rev. B 84 (2011) 224121.
[15] V. Panchal, S. López-Moreno, D. Santamaría-Pérez, D. Errandonea, F.J. Manjón, P. Rodríguez-Hernandez, A. Muñoz, S.N. Achary, A.K. Tyagi, Zircon to monazite phase transition in $CeVO_4$: x-ray diffraction and Raman-scattering measurements, Phys. Rev. B 84 (2011) 024111.
[16] D. Errandonea, S.N. Achary, J. Pellicer-Porres, A.K. Tyagi, Pressure-induced transformations in $PrVO_4$ and $SmVO_4$ and isolation of high-pressure metastable phases, Inorg. Chem. 52 (2013) 5464–5469.
[17] D. Errandonea, F.J. Manjón, A. Muñoz, P. Rodríguez-Hernández, V. Panchal, S.N. Achary, A.K. Tyagi, High-pressure polymorphs of $TbVO_4$: a Raman and ab initio study, J. Alloy. Compd. 577 (2013) 327–335.
[18] D. Errandonea, C. Popescu, S.N. Achary, A.K. Tyagi, M. Bettinelli, In situ high-pressure synchrotron X-ray diffraction study of the structural stability in $NdVO_4$ and $LaVO_4$, Mater. Res. Bull. 50 (2014) 279–284.
[19] A.B. Garg, D. Errandonea, P. Rodriguez-Hernandez, S. Lopez-Moreno, A. Munoz, C. Popescu, High-pressure structural behaviour of $HoVO_4$: combined XRD experiments and ab initio calculations, J. Phys.: Condens. Matter 26 (2014) 265402.
[20] W. Paszkowicz, O. Ermakova, J. Lopez-Solano, A. Mujica, A. Munoz, R. Minikayev, C. Lathe, S. Gierlotka, I. Nikolaenko, H. Dabkowska, Equation of state of zircon- and scheelite-type dysprosium orthovanadates: a combined experimental and theoretical study, J. Phys.: Condens. Matter 26 (2014) 025401.
[21] A.B. Garg, D. Errandonea, High-pressure powder x-ray diffraction study of $EuVO_4$, J. Solid State Chem. 226 (2015) 147–153.
[22] H. Yuan, K. Wang, C. Wang, B. Zhou, K. Yang, J. Liu, B. Zou, Pressure-induced phase transformations of zircon-type $LaVO_4$ nanorods, J. Phys. Chem. C 119 (2015) 8364–8372.
[23] C. Popescu, A.B. Garg, D. Errandonea, J.A. Sans, P. Rodriguez-Hernandez, S. Radescu, A. Munoz, S.N. Achary, A.K. Tyagi, Pressure-induced phase transformation in zircon-type orthovanadate $SmVO_4$ from experiment and theory, J. Phys.: Condens. Matter 28 (2016) 035402.
[24] E. Bandiello, D. Errandonea, J. González-Platas, Pc Rodríguez-Hernández, A. Muñoz, M. Bettinelli, C. Popescu, Phase behavior of $TmVO_4$ under hydrostatic compression: an experimental and theoretical study, Inorg. Chem. 59 (2020) 4882–4894.
[25] T. Marqueo, D. Errandonea, J. Pellicer-Porres, D. Martinez-Garcia, M. Bettinelli, High-pressure polymorphs of gadolinium orthovanadate: X-ray diffraction, Raman spectroscopy, and ab initio calculations, Phys. Rev. B 100 (2019) 064106.
[26] J. Ruiz-Fuertes, D. Martínez-García, Ts Marqueño, D. Errandonea, S.G. MacLeod, T. Bernert, E. Haussühl, D. Santamaria-Perez, J. Ibáñez, A. Mallavarapu, High-pressure high-temperature stability and thermal equation of state of zircon-type erbium vanadate, Inorg. Chem. 57 (2018) 14005–14012.
[27] K. Kishimoto, T. Ishikura, H. Nakamura, Y. Wakabayashi, T. Kimura, Antiferroelectric lattice distortion induced by ferroquadrupolar order in $DyVO_4$, Phys. Rev. B 82 (2010) 012103.
[28] A. Midya, N. Khan, D. Bhoi, P. Mandal, Giant magnetocaloric effect in antiferromagnetic $DyVO_4$ compound, Phys. B Condens. Matter 448 (2014) 43–45.
[29] R.J. Elliott, G.A. Gehring, A.P. Malozemoff, S.R.P. Smith, W.S. Staude, R.N. Tyte, Theory of co-operative Jahn-Teller distortions in $DyVO_4$ and $TbVO_4$ (Phase transitions), J. Phys. C: Solid State Phys. 4 (1971) L179–L183.
[30] R.T. Harley, W. Hayes, S.R.P. Smith, Raman study of phase transitions in rare earth vanadates, Solid State Commun. 9 (1971) 515–517.
[31] Y. He, J. Cai, T. Li, Y. Wu, Y. Yi, M. Luo, L. Zhao, Synthesis, characterization, and activity evaluation of $DyVO_4$/g-C_3N_4 composites under visible-light irradiation, Ind. Eng. Chem. Res. 51 (2012) 14729–14737.
[32] F. Zhan, Y. Yang, W. Li, J. Li, W. Liu, Y. Li, Q. Chen, Preparation of $DyVO_4$/WO_3 heterojunction plate array films with enhanced photoelectrochemical activity, RSC Adv. 6 (2016) 10393–10400.
[33] H. Li, Y. Liu, Y. Cui, W. Zhang, C. Fu, X. Wang, Facile synthesis and enhanced visible-light photoactivity of $DyVO_4$/g-C_3N_4I composite semiconductors, Appl. Catal. B: Environ. 183 (2016) 426–432.
[34] S.J. Duclos, A. Jayaraman, G.P. Espinosa, A.S. Cooper, R.G.M. Sr, Raman and optical absorption studies of the pressure-induced zircon to scheelite structure transformation in $TbVO_4$ and $DyVO_4$, J. Phys. Chem. Solids 50 (1989) 769–775.
[35] N.N. Patel, A.B. Garg, S. Meenakshi, B.N. Wani, S.M. Sharma , High pressure raman scattering study on the phase stability of $DyVO_4$, in: American Institute of Physics Conference Series, 2011, pp. 99–100.
[36] J.P. Bastide, Systématique simplifiée des composés ABX_4 (X= O^{2-}, F^-) et evolution possible de leurs structures cristallines sous pression, J. Solid State Chem. 71 (1987) 115–120.
[37] D. Errandonea, F.J. Manjón, Pressure effects on the structural and electronic properties of ABX_4 scintillating crystals, Prog. Mater. Sci. 53 (2008) 711–773.
[38] D. Errandonea, Exploring the properties of MTO_4 compounds using high-pressure powder x-ray diffraction, Cryst. Res. Technol. 50 (2015) 729–736.
[39] O. Ermakova, W. Paszkowicz, J. López-Solano, A. Muñoz, H. Dabkowska, Experimental and theoretical study of Zircon and Scheelite phases of $DyVO_4$, Acta Phys. Pol. 121 (2012) 920–924.
[40] H. Mao, J.A. Xu, P. Bell, Calibration of the ruby pressure gauge to 800 kbar under quasi-hydrostatic conditions, J. Geophys. Res.: Solid Earth 91 (1986) 4673–4676.
[41] M. Yokoo, N. Kawai, K.G. Nakamura, K.I. Kondo, Y. Tange, T. Tsuchiya, Ultrahigh-pressure scales for gold and platinum at pressures up to 550 GPa, Phys. Rev. B 80 (2009) 104114.
[42] A.P. Hammersley, FIT2D: a multi-purpose data reduction, analysis and visualization program, J. Appl. Crystallogr. 49 (2016) 646–652.
[43] C. Prescher, V.B. Prakapenka, DIOPTAS: a program for reduction of two-dimensional X-ray diffraction data and data exploration, High Press. Res. 35 (2015) 223–230.
[44] B.H. Toby, EXPGUI, a graphical user interface for GSAS, J. Appl. Crystallogr. 34 (2001) 210–213.
[45] D. Errandonea, A.B. Garg, Recent progress on the characterization of the high-pressure behaviour of AVO_4 orthovanadates, Prog. Mater. Sci. 97 (2018) 123–169.
[46] S. Klotz, J.C. Chervin, P. Munsch, G. Le, Hydrostatic limits of 11 pressure transmitting media, J. Phys. D: Appl. Phys. 42 (2009) 075413.
[47] F. Birch, Finite elastic strain of cubic crystals, Phys. Rev. B 71 (1947) 809–824.
[48] F. Birch, Finite strain isotherm and velocities for single-crystal and polycrystalline NaCl at high pressures and 300 K, J. Geophys. Res.: Solid Earth 83 (1978) 1257–1268.
[49] A.B. Garg, D. Errandonea, P. Rodriguez-Hernandez, A. Munoz, $ScVO_4$ under non-hydrostatic compression: a new metastable polymorph, J. Phys.: Condens. Matter 29 (2017) 055401.